



Observation of long-lived excitons in InAs quantum dots under thermal redistribution temperature

Chun Cheng, Sheng-Di Lin*, Chien-Hung Pan, Chien-Hung Lin, Ying-Jhe Fu

Department of Electronics Engineering, National Chiao Tung University, 1001 Ta Hsueh Road, Hsinchu 300, Taiwan

ARTICLE INFO

Article history:

Received 30 January 2012

Accepted 6 March 2012

Available online 9 March 2012

Communicated by V.M. Agranovich

Keywords:

Quantum dot

Time-resolved photoluminescence

Spin-flip

ABSTRACT

We study the temperature-dependent time-resolved photoluminescence (TRPL) of self-assembled InAs quantum dots (QDs). Under low excitation power, a surprisingly long PL decay time is observed at about 60 K, under the thermal redistribution temperature. The long decay time decreases with increasing excitation power but is nearly independent of the detection energy of TRPL measurements. A model considering the spin relaxation through the excited excitonic state is proposed to quantitatively explain the unusual phenomena. The rate equation analysis indicates that the observation of long-lived excitons is caused by the shortened spin-flip time.

© 2012 Elsevier B.V. All rights reserved.

1. Introduction

Self-assembled semiconductor quantum dots (QDs) have been a central topic for two decades. The potential applications on optoelectronic devices and quantum information processing are promising because of their defect-free quality and superior optical properties [1–3]. Recently, the dark excitons in QDs received growing attention due to the possibility of using them as spin storage and qubits [4–6]. To process spin information using QD, it is essential to study the interplay between bright and dark excitons and many related works have been reported recently [5–9]. In this Letter, we report the first observation of long-lived exciton in individual InAs QDs, which is strongly related to the optically-inactive dark exciton. Revealing by the proposed model and by the numerical analysis of rate equations, we claim that the very long PL decay time is caused by the thermal-induced spin-flip which turns dark excitons into bright ones. This work provides a piece to understand the complex dynamics in QDs and paves the way of using QDs as a spin qubit at elevated temperature.

To study the carrier dynamics in QDs, temperature-dependent TRPL is one of the most common methods. The temperature-dependent exciton dynamics in InAs QDs ensembles has been extensively studied but its physical mechanism in whole temperature range is not well understood [8]. Typically, for InAs QDs, the measured carrier decay time keeps nearly constant at temperatures less than 100 K. In middle temperature range (~100–200 K),

a moderate rise of decay time is commonly observed, owing to the thermal redistribution among QDs [10,11]. That is, when the carrier emission/re-capture time is comparable with the recombination time of ground states, the thermal redistribution among QDs begins so the thermal equilibrium between individual QDs gradually builds up. As a result, the PL decay time increases and the full-width-half-maximum (FWHM) of PL spectra decreases. At near room temperature, the non-radiative recombination becomes dominant so a rapid decrease of carrier lifetime was observed in most samples [10,12–16]. In this work, we present the first observation of an anomalous behavior of long-lived excitons in the temperature range of 50–75 K. A three-level model, including bright, dark, and hot excitonic states is proposed to explain the unusual phenomena. A consistent fit between the theory and the experiment is obtained with the rate equation simulation, which reveals the important role of hot excitonic state in spin relaxation of carriers in QDs.

2. Sample growth and measurement setup

The QDs were grown by a solid-source molecular beam epitaxy system (Varian Gen II) on (100) GaAs substrate. More than 20 samples were studied but we focus on two representative samples here, noted as sample A (LM3572) and sample B (LM4682). The QDs were centrally embedded in 300 nm GaAs and sandwiched with two AlGaAs confinement layers. For the QDs growth, the InAs nominal thickness, growth rate and substrate temperature are 2.4 (3.0) monolayers (MLs), 0.05 (0.05) ML/s and 500 (480) °C for sample A (sample B), respectively. The growth ended with an uncapped QDs layer grown at the same condition for surface morphology

* Corresponding author. Tel.: +886 3 5131240; fax: +886 3 5724361.

E-mail address: sdlin@mail.nctu.edu.tw (S.-D. Lin).

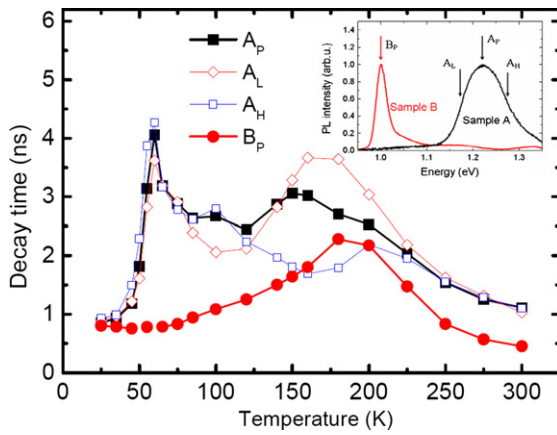


Fig. 1. (Color online.) Temperature-dependent PL decay times detected at the peak energies of samples A and B (solid symbols), as well as those detected at subgroups QDs of sample A (open symbols). Inset: the PL spectra of two samples and the indication of detection energies.

observation. All layers were undoped. The QDs area density measured with atomic force microscopy is about $8.0 \times 10^{10} \text{ cm}^{-2}$ for sample A and about $6.0 \times 10^{10} \text{ cm}^{-2}$ for sample B. Continuous-wave low-temperature ($\sim 20 \text{ K}$) PL measurements show that the PL ground state energy and FWHM of sample A (sample B) are 1.21 eV (1.09 eV) and 95 meV (33 meV), respectively. To perform TRPL measurements, the samples were excited with a pulsed diode laser ($\lambda = 780 \text{ nm}$, pulse width $\sim 50 \text{ ps}$ and repetition rate = 10 MHz) with a spot size of about $60 \mu\text{m}$. By considering the spot size and the net absorption of GaAs matrix, the number of photo-generated electron-hole pairs per dot is less than 0.13 at the average excitation power of $2 \mu\text{W}$ for sample A (QDs' area density = $8.0 \times 10^{10} \text{ cm}^{-2}$). The PL were dispersed by a monochromator and then detected by an InGaAs photo-multiplier tube (PMT) using time-correlated single photon counting technique. The time resolution of TRPL system is about 0.3 ns, limited by the response time of InGaAs PMT. At each temperature, the PL spectra were taken prior to the TRPL measurements to decide the detection wavelength. The PL decay time is extracted by fitting the measured decay curves with the bi-exponential function below. For clarity, we define the fast part of the decay curve as the PL decay time (i.e. the smaller τ , denoted as τ_1)

$$I_{\text{PL}}(t) = A_1 \exp(-t/\tau_1) + A_2 \exp(-t/\tau_2). \quad (1)$$

3. Result and discussion

Fig. 1 shows the extracted PL decay times from 25 to 300 K. The excitation power of sample A (sample B) is $20 \mu\text{W}$ ($25 \mu\text{W}$). First, the decay times of sample B (B_p) exhibit the typical temperature dependence but those of sample A detected at peak wavelength (A_p) shows an unusual spike between 50 and 75 K. A surprising lone decay time of about 4.0 ns is obtained. To see the decay times of the subgroups of the QDs ensemble, we also plotted the decay time of sample A detected at the energies lower (A_L) and higher (A_H) than its peak energy, by the half of FWHM. In the middle temperature range (125–225 K), the decay times of these three subgroup QDs have different trends due to thermal redistribution among QDs. This is exactly what we expected as mentioned above. The carriers in smaller QDs can escape the confinement before radiative recombination and re-capture by the larger QDs. Obviously, in this temperature range, the thermal redistribution of carriers causes the different decay times between QDs' subgroups. Nevertheless, the long decay time at 60 K appears with all of the three subgroups. It reveals that the increase of decay

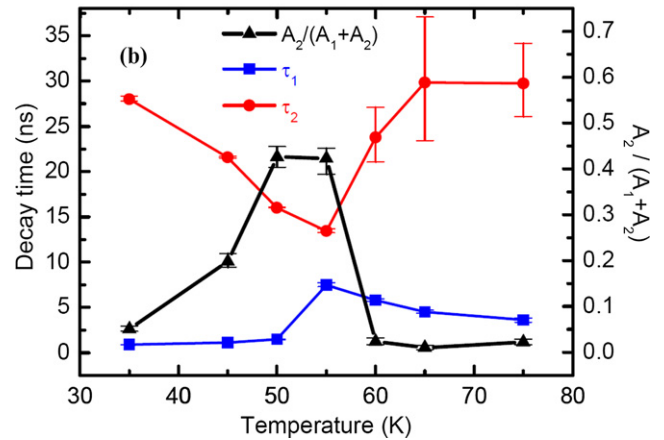
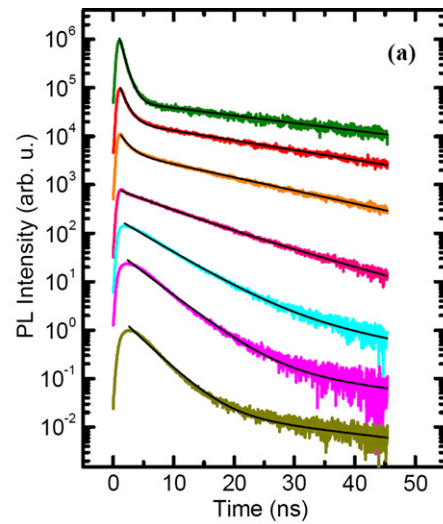


Fig. 2. (Color online.) (a) Measured PL time traces of sample A for $T = 35\text{--}75 \text{ K}$. At each temperature, the black line is a fit of bi-exponential function to the data. (b) The fast and slow decay times and the amount ratio of slow part, extracted from (a).

time is irrelevant with the carrier transfer among QDs thereby it occurs in all individual QDs. In addition, the integrated PL intensity in 25–100 K is nearly constant (within $\pm 10\%$) so the non-radiative recombination is probably unrelated to the unusual behavior.

To see the long decay time in detail, we show the time traces of sample A from 35 to 75 K under the excitation power of $2 \mu\text{W}$ in **Fig. 2(a)**. Note that the vertically-shifted PL intensity is plotted in logarithmic scale so their slopes are proportional to the inverse of decay times. At $T = 35 \text{ K}$, a typical bi-exponential decay ($\tau_1 \sim 0.8 \text{ ns}$, $\tau_2 \sim 32 \text{ ns}$) is clearly seen. The fast one comes from the bright exciton recombination and the slow one is attributed to the spin-flip of dark excitons [5–9]. In 35–50 K, the slopes of fast decay decrease with increasing temperatures. The longest τ_1 is seen at 55 K, which is caused by the replacement of the fast decay part with the slow one. The numerical fitting is also plotted in **Fig. 2(a)** with detailed results shown in **Fig. 2(b)**. With raising temperatures, τ_1 increases and τ_2 reduces, where they become closest at 55 K. The replacement of the fast part with the slow one is clearly revealed by the A_2 ratio, defined as $A_2/(A_1 + A_2)$, which reaches its peak value also around 55 K. For $T > 55 \text{ K}$, the slow part is negligible. Accordingly, we can say that the decays are basically two components at temperatures less than about 55 K then they become mono-exponential decay for higher temperatures. That is, the fast one dominates at low temperatures but, with

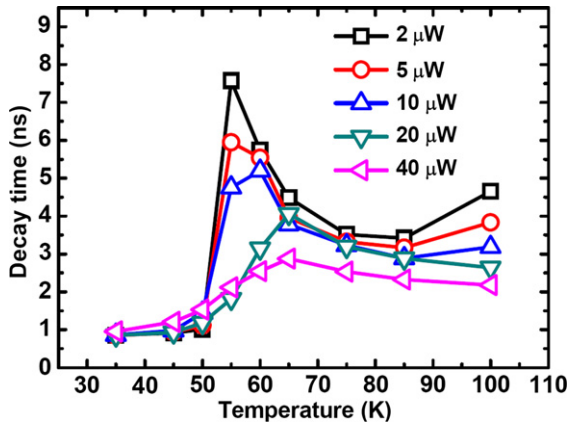


Fig. 3. (Color online.) Temperature-dependent PL decay times measured with various excitation powers.

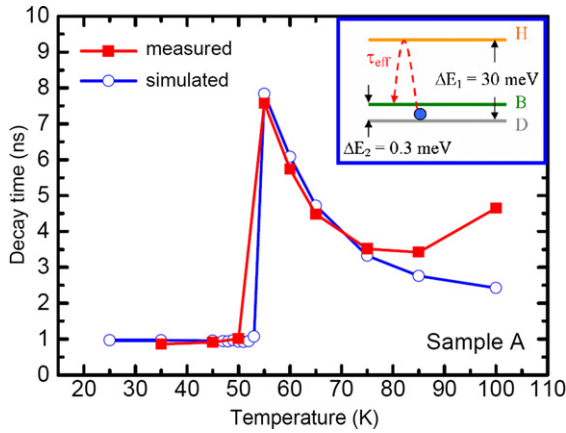


Fig. 4. (Color online.) Measured and simulated PL decay time of sample A. Inset: the schematic of proposed three-excitonic-states model.

increasing temperatures, the slow one fastens and then takes over at about 55 K.

We have also performed power-dependent TRPL measurement on sample A, as shown in Fig. 3. It is clearly observed that the anomalous spike becomes much more significant as the excitation power decreases. At the lowest excitation power in our measurement (2 μW), the peak decay time is as high as 7.6 ns. As the excitation power increases, the spike gradually flattens out. This can be easily understood as follows. The increasing excitation power enhances the possibility of bi-exciton generation and the bi-exciton decay leaves the exciton in bright state so the dark state is less occupied. As a result, the slow decay arising from the spin-flip of dark excitons has little chance to replace the fast one when the temperature increases.

To explain the unusual behavior quantitatively, we propose a three-level model including hot, bright and dark excitonic states (see the inset of Fig. 4). The energy difference between bright and dark excitonic states (ΔE_2) is of hundreds μeV [7,17,18]. Comparing with the radiative recombination time ($\tau_r \sim 1$ ns) of bright exciton, the spin-flip time between dark and bright states is very long at low temperature ($\tau_{\text{spin-flip}} \sim 100$ ns) [9,17,18]. The effective hot excitonic state could arise from the exciton formed by a hole (an electron) at the excited state and an electron (a hole) at the ground state, as well as other combinations of higher states. The relaxation time to either bright or dark state, noted as τ_{relax} (\sim a few ps), is believed to be much faster than τ_r . Based on the model, we performed calculation with the rate equation in the following:

$$\begin{aligned} \frac{dN_b}{dt} &= -\left[\frac{N_b}{\tau_r} + \frac{N_b}{\tau_{bd}} \left(1 - \frac{N_d}{n_d} \right) + \frac{N_b}{\tau_{bh}} \left(1 - \frac{N_h}{n_h} \right) \right] \\ &\quad + \left[\frac{N_d}{\tau_{db}} \left(1 - \frac{N_b}{n_b} \right) + \frac{N_h}{\tau_{hb}} \left(1 - \frac{N_b}{n_b} \right) \right], \\ \frac{dN_d}{dt} &= -\left[\frac{N_d}{\tau_{db}} \left(1 - \frac{N_b}{n_b} \right) + \frac{N_d}{\tau_{dh}} \left(1 - \frac{N_h}{n_h} \right) \right] \\ &\quad + \left[\frac{N_b}{\tau_{bd}} \left(1 - \frac{N_d}{n_d} \right) + \frac{N_h}{\tau_{hd}} \left(1 - \frac{N_d}{n_d} \right) \right], \\ \frac{dN_h}{dt} &= -\left[\frac{N_h}{\tau_{hb}} \left(1 - \frac{N_b}{n_b} \right) + \frac{N_h}{\tau_{hd}} \left(1 - \frac{N_d}{n_d} \right) \right] \\ &\quad + \left[\frac{N_b}{\tau_{bh}} \left(1 - \frac{N_h}{n_h} \right) + \frac{N_d}{\tau_{dh}} \left(1 - \frac{N_h}{n_h} \right) \right]. \end{aligned} \quad (2)$$

The variables N_i and n_i ($i = b, d, h$) are the occupation number and the maximum allowed number of excitons for each state, respectively. τ_{ij} is the transition time between states i and j . Because the energy difference between the bright and dark states (ΔE_2) is much smaller than the thermal energy $k_B T$ at $T = 50$ K, we assume that $\tau_{db} = \tau_{bd} = \tau_{\text{spin-flip}}$, $\tau_{hb} = \tau_{hd} = \tau_{\text{relax}}$ but $\tau_{bh} = \tau_{hb} \times e^{\Delta E_1/k_B T}$. With the following parameters, $\tau_r = 1$ ns, $\tau_{\text{relax}} = 10$ ps, $\tau_{\text{spin-flip}} = 30$ ns, $\Delta E_1 = 30$ meV, $\Delta E_2 = 0.3$ meV, and with an odd but necessary unbalanced initial condition of $N_d(0) = 4N_b(0)$, where $N_d(0)$ and $N_b(0)$ are the initial occupation numbers of dark and bright states, respectively, we can fit the simulated results with the measured ones very well below 80 K (see Fig. 4). The discrepancy at higher temperatures could be because of the slight involvement of thermal redistribution between QDs.

Here we give an intuitive explanation to the observation. At the lowest temperature, the dark excitons can only become the bright ones with the slow spin-flip rate. However, with increasing temperatures, there is an additional path as sketched in the inset of Fig. 4. Dark excitons can turn into bright ones through the hot excitonic states. This path has an effective transition time τ_{eff} , expressed as follows:

$$\tau_{\text{eff}} = \tau_{\text{relax}} \times \exp(\Delta E_1/k_B T). \quad (3)$$

When the thermal energy is much smaller than the energy spacing between dark and hot excitonic states (i.e. $k_B T \ll \Delta E_1$), τ_{eff} is much longer than τ_r and the exciton supply through this additional path is negligible so $\tau_1 = \tau_r$. However, when $k_B T$ is large enough to make τ_{eff} is comparable with τ_r , the exciton comes from the additional path could compensate the consumption of radiative recombination so the measured decay time is significantly prolonged. For even higher temperatures, the additional path becomes even more efficient so the decay time is limited by τ_r again. Besides, in the measured more than 20 samples, the long decay time was obtained with about one third of them. No obvious correlation between the growth conditions and the unusual behavior is spotted. The sample dependence of observing the long decay time could probably be understood by Eq. (3). The τ_{eff} is governed by two parameters, τ_{relax} and ΔE_1 . They are strongly correlated because the energy spacing between two states could affect the relaxation time between them [2]. Accordingly, to observe the effect, proper values of these two parameters could be quite important. Of course, the size-dependent energy difference between dark and bright states could also be a factor [18] but further investigations are certainly needed to clarify this issue.

4. Conclusion

In conclusion, we presented the first observation of long-lived exciton in individual InAs QDs. The rate equation analysis indicates

that the effective spin-flip time could become comparable with the radiative recombination time when the thermal-induced spin-flip is fastened. Our work is useful for using dark excitons as spin storage at elevated temperatures.

Acknowledgements

This work was supported by NSC and MOE in Taiwan. The equipment support from CNST at NCTU is appreciated. We thank Profs. C.P. Lee, W.H. Chang and S.J. Cheng for their inspiring discussions.

References

- [1] D. Bimberg, M. Grundmann, N.N. Ledentsov, *Quantum Dot Hetero-Structures*, Wiley, New York, 1998.
- [2] D.J. Mowbray, M.S. Skolnick, *J. Phys. D: Appl. Phys.* 38 (2005) 2059.
- [3] C.H. Wu, Y.G. Lin, S.L. Tyan, S.D. Lin, C.P. Lee, *Chinese J. Phys.* 43 (2005) 847.
- [4] A. Imamoglu, D.D. Awschalom, G. Burkard, D.P. DiVincenzo, D. Loss, M. Sherwin, A. Small, *Phys. Rev. Lett.* 83 (1999) 4204.
- [5] O. Labeau, P. Tamarat, B. Lounis, *Phys. Rev. Lett.* 90 (2003) 257404.
- [6] J.M. Smith, P.A. Dalgarno, R.J. Warburton, A.O. Govorov, K. Karrai, B.D. Gerardot, P.M. Petroff, *Phys. Rev. Lett.* 94 (2005) 197402.
- [7] M. Bayer, G. Ortner, O. Stern, A. Kuther, A.A. Gorbunov, A. Forchel, P. Hawrylak, S. Fafard, K. Hinzer, T.L. Reinecke, S.N. Walck, J.P. Reithmaier, F. Klopff, F. Schäfer, *Phys. Rev. B* 65 (2002) 195315.
- [8] T. Kümmell, S.V. Zaitsev, A. Gust, C. Kruse, D. Hommel, G. Bacher, *Phys. Rev. B* 81 (2010) 241306(R).
- [9] J. Johansen, B. Julsgaard, S. Stobbe, J.M. Hvam, P. Lodahl, *Phys. Rev. B* 81 (2010) 081304(R).
- [10] W. Yang, R.R. Lowe-Webb, H. Lee, P.C. Sercel, *Phys. Rev. B* 56 (1997) 13314.
- [11] S. Sanguinetti, M. Henini, M. Grassi Alessi, M. Capizzi, P. Frigeri, S. Franchi, *Phys. Rev. B* 60 (1999) 8276.
- [12] G. Wang, S. Fafard, D. Leonard, J.E. Bowers, J.L. Merz, P.M. Petroff, *Appl. Phys. Lett.* 64 (1994) 2815.
- [13] D.I. Lubyshev, P.P. Gonzalez-Borrero, E. Marega Jr., E. Petitprez, N. La Scala Jr., P. Basmaji, *Appl. Phys. Lett.* 68 (1996) 205.
- [14] H. Yu, S. Lycett, C. Roberts, R. Murray, *Appl. Phys. Lett.* 69 (1996) 4087.
- [15] A. Fiore, P. Borri, W. Langbein, J.M. Hvam, U. Oesterle, R. Houdre, R.P. Stanley, M. Illegems, *Appl. Phys. Lett.* 76 (2000) 3430.
- [16] J. Gomis, J. Martinez-Pastor, B. Alén, D. Granados, J.M. Garcia, P. Roussignol, *Eur. Phys. J. B* 54 (2006) 471.
- [17] M. Paillard, X. Marie, P. Renucci, T. Amand, A. Jbeli, J.M. Gérard, *Phys. Rev. Lett.* 86 (2001) 1634.
- [18] Y.H. Liao, J.I. Climente, S.J. Cheng, *Phys. Rev. B* 83 (2011) 165317.